Computer Simulation of Grain Growth by the Phase Field Model. Effect of Interfacial Energy on Kinetics of Grain Growth

Yoshihiro Suwa¹ and Yoshiyuki Saito²

¹ Research Center for Advanced Science and Technology, The University of Tokyo, Tokyo 153-8904, Japan

Numerical simulations of grain growth based on the phase field method were performed in order to investigate effect of interfacial energy on kinetics of growth. From the theoretical analysis of the evolution equation with the Ginzburg-Landua type free energy functional, It is known that the gradient energy coefficient κ , and a parameter γ in a local free energy function affects interfacial energy of a materials. Numerical simulation results indicate that the average size is proportional to the square root of time and after a short transient time, the grain size distribution and the grain side distribution functions become time-independent. These results are in good agreement with these obtained by the mean field theory and the Monte Carlo simulation. Growth rate becomes larger with the increase of κ and growth rate becomes smaller with the increase of γ . These results are in good agreement with these obtained by conventional theories.

(Received May 29, 2003; Accepted September 3, 2003)

Keywords: grain growth, computer simulation, phase field model, interfacial energy

1. Introduction

Control of microstructure of a polycrystalline material is one of most important factors that determines properties of the materials such as strength, toughness, electrical conductivity and magnetic susceptibility. Understanding of kinetics of grain growth is thus of fundamental importance, not only for its intrinsic interest, but also for its technological significance. 1,2) Due to the difficulty of incorporating topological features into analytical theories of grain growth directly^{3–5)} there has been increasing interest in the use of computer simulations to study grain growth. A variety of models have been proposed during the past decades. ^{6–12)} The common feature of these models is that the grain boundaries are described as sharp interfaces with zero thickness. On one hand, this assumption has an advantage in modeling for its simplicity, on the other hand, however it has the disadvantage in predicting microstructure of practical materials. Recently, a rather different model for the microstructural evolution, in which interfaces are assumed to be diffuse with finite thickness, was proposed. 13-17)

This model, the phase field model, is based on the Onsager's linear irreversible thermodynamics. It has been extensively applied to simulation of temporal and spatial evolution of microstructure. This model represents temporal evolutions in the chemical, crystallographic and structural fields. These state variables are called field variables. The polycrystalline microstructure is described by a set of orientation field variables; $\eta_1(r), \eta_2(r), \ldots, \eta_p(r)$.

In this paper, we will deal with single-phase polycrystal-line materials. The phase field model has been successfully aplied to grain growth in 2-dimensional and 3-dimensional systems. The interfacial energy of a material is related to parameters in fundamental equations of the phase field models, ie. the gradient energy coefficient κ , and a parameter in a local free energy function γ . In order to investigate the effect of interfacial energy on kinetics of grain growth, computer simulations were performed under conditons with various κ and γ .

2. Model

2.1 Phase field model

In the phase field model for the grain growth of polycrystalline materials, microstructure of polycrystalline materials is described by set of orientation field variables, $\eta_1(r), \eta_2(r), \ldots, \eta_p(r)$, where $\eta_i(r)$ ($i=1,2,\ldots,p$) are called orientation field variables that distinguish different orientations of grains and p is the number of possible orientations. A schematic microstructure represented by orientation fields in 2-D is shown in Fig. 1. Within the grain labeled by η_1 , the absolute value for η_1 is 1 while all other η_i for $i \neq 1$ is zero. Across the grain boundaries between the grain η_1 , and its neighbor grains, the absolute value of η_1 changes continuously from 1 to 0. The schematic profiles of η_1 and η_2 across the grain boundary between the grain η_1 and η_2 are shown in Fig. 2. All other field variables this grain boundary having zero values. According to Cahn's and

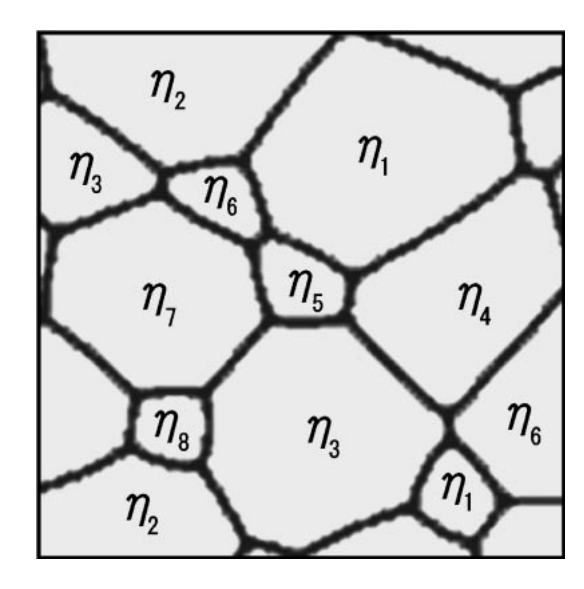


Fig. 1 A schematic illustration of a microstructure described using orientation variables.

² Department of Materials Science and Engineering, Waseda University, Tokyo 169-8555, Japan

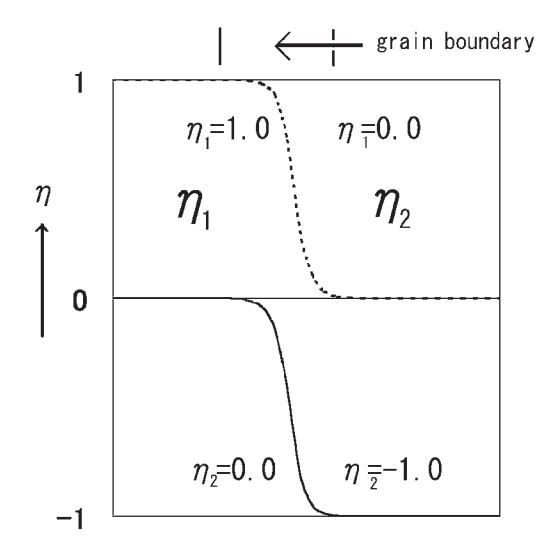


Fig. 2 Schematic illustration of two orientation variables across a flat grain boundary.

Hilliard's treatment, ¹⁸⁾ the total free energy functional of an inhomogeneous system is given by

$$F = \int \left[f_0(\eta_1(r), \eta_2(r), \dots, \eta_p(r)) + \sum_{k=1}^p \frac{\kappa}{2} (\nabla \eta_i(r))^2 \right] d^3r$$

$$(i = 1, 2, \dots, p) \tag{1}$$

where f_0 is the local free energy density which is a function of orientation field variables, $\eta_i(r)$, and κ is the gradient energy coefficient. The spatial and temporal evolutions of orientation field variables are described by the time-dependent Ginzburg-Landau equations for nonconserved order parameter.

$$\frac{\partial \eta_i(r,t)}{\partial t} = -L_i \frac{\delta F}{\delta n \cdot (r,t)} \tag{2}$$

where L_i are the Onsager's phenomenological coefficients. We used the Ginzburg-Landau type free energy density functional for the present simulation

$$f_0(\eta_1(r), \eta_2(r), \dots, \eta_p(r)) = \sum_{i=1}^p \left(-\frac{\alpha}{2} \eta_i^2 + \frac{\beta}{4} \eta_i^4 \right) + \gamma \sum_{i=1}^p \sum_{i=1}^p \eta_i^2 \eta_j^2$$
(3)

where α , β and γ are phenomenological parameters. The only requirement for f_0 is that it has 2p minima with equal well depth at $(\eta_1, \eta_2, \ldots, \eta_p) = (1, 0, \ldots, 0), (0, 1, \ldots, 0), \ldots, (0, 0, \ldots, 1), (-1, 0, \ldots, 0), (0, -1, \ldots, 0), \ldots, (0, 0, \ldots, -1).$ Therefore, γ has to be greater than $\beta/2$ when we assume $\alpha = 1, \beta = 1$. As will be shown in section 3.1, the gradient energy coefficient κ and parameter γ are considered to effect the interfacial energy.

2.2 Numerical solution to the kinetic equations

For the purpose of simulating the grain growth kinetics, the set of kinetic eq.(2) have to be solved numerically by discretizing them in space and time. In this paper, the Laplacian is discretized by the following equation,

$$\nabla^{2} \eta_{i} = \frac{1}{(\Delta x)} \left[\frac{1}{2} \sum_{j} (\eta_{j} - \eta_{i}) + \frac{1}{4} \sum_{k} (\eta_{k} - \eta_{i}) \right]$$
(4)

where Δx is the discretizing grid size, j represents the first nearest neighbors of site i, and k represents the second nearest neighbors. For discretization with respect to time, we used the simple explicit Euler equation,

$$\eta_i(t + \Delta t) = \eta_i + \frac{d\eta_i}{dt} \times \Delta t$$
(5)

where Δt is the time step for integration. The numerical simulation started from a liquid-like phase by assuming small random values to all field variables between -0.001 and 0.001. Periodic boundary conditions were applied.

2.3 Condition of simulation

All simulations were performed in 2-D systems. The following numerical parameters were used in the kinetic equations: $\alpha=1.0$, $\beta=1.0$, $L_i=1.0$ ($i=1,2,\ldots,p$). The values of γ and κ were varied from 0.5 to 3.0 and from 0.5 to 3.5, respectively. Default value of γ and κ were $\gamma=1.0, \kappa=2.0$ ($i=1,2,\ldots,p$). The grid sizes along both Cartesian coordinate axes were chosen as $\Delta x=2.0$, and the time step for integration, $\Delta t=0.1$. Periodic boundary conditions were applied. The system sizes cells were chosen as 512x512 grid points to obtain distribution functions. Since, for small p, microstructural coarsening was dominated by coalescence between grains with the same orientation, the number of field variables was chosen as p=48.

As mentioned in the last section, the initial condition was specified by assigning small random values to all field variables at every grid point, $e.g. -0.001 < \eta_i < 0.001$, simulating a liquid-like phase. All kinetic data were obtained by averaging over several independent runs starting with different initial conditions. A typical simulation time for a system with 512x512 grid points and 10000 time steps requires about 7 h on a computer with Alpha-21264(666Mhz) processor.

3. Results and discussion

3.1 Evaluation of the Interfacial Energy

Let us relate to parameters κ and γ to interfacial energy with use of a simple model. As we described in chapter 2, the total free energy functional of an inhomogeneous system F is given by

$$F = \int \left[f_0(\eta_1(r), \eta_2(r), \dots, \eta_p(r)) + \sum_{k=1}^p \frac{\kappa}{2} (\nabla \eta_i(r))^2 \right] d^3r$$

$$(i = 1, 2, \dots, p)$$

We can express the total free energy functional as follows:

$$F = \int \left[\sum_{i=1}^{p} \left(-\frac{\alpha}{2} \eta_i^2 + \frac{\beta}{4} \eta_i^4 \right) + \gamma \sum_{i=1}^{p} \sum_{j=1}^{p} \eta_i^2 \eta_j^2 + \sum_{k=1}^{p} \frac{\kappa}{2} (\nabla \eta_i(r))^2 \right] d^3r$$

$$(i = 1, 2, \dots, p) \tag{6}$$

Let us consider the stationary solution which $\delta F/\delta \eta_i = 0.^{19}$. Since this solution implys the lowest saddle point which connects one valley of the free energy functional with the other valley, it is called saddle point solution. We consider an analytical solution $\eta_i(r)$ for a flat interface by assuming that the saddle point exists in yz-plane (perpendicular to x-axis). Substitution of eq.(4) into variational functional $\delta F/\delta \eta_i = 0$ gives

$$\frac{\delta F}{\delta \eta_i} = \left(-\alpha + 2\gamma \sum_{j \neq i}^p \eta_j^2\right) \eta_i + \beta \eta_i^3 - \kappa \frac{d^2 \eta_i}{dx^2} = 0 \quad (7)$$

Multiplying both sides of eq.(5) by $d\eta/dx$, and integrate the left side from 0 to x, we have

$$-\frac{1}{2}\epsilon\eta_i^2 + \frac{1}{4}\beta\eta_i^4 - \frac{1}{2}\kappa \left(\frac{d^2\eta_i}{dx^2}\right)^2 = -\frac{\epsilon^2}{4\beta}$$
 (8)

where $\epsilon = \alpha - 2\gamma \sum_{j \neq i}^p \eta_j^2$. To get the value of right-hand side,

we assume that $\eta_i(x)$ reaches the equilibrium value, $\pm \sqrt{\epsilon/\beta}$ at $x \to \pm \infty$. In this case we can get the following solutions:

$$\eta_{i0}(x) = \pm \sqrt{\frac{\epsilon}{\beta}} \tanh\left(\sqrt{\frac{\epsilon}{2\kappa}}x\right)$$
(9)

We can express surface energy σ as follows: ¹⁸⁾

$$\sigma = \int \kappa \left(\frac{d\eta}{dx}\right)^2 dx \tag{10}$$

If all other field variables than i and j are zero at and around grain boundaries between the grain i, the grain j, substitution of the flat interface solution eq.(7) into eq.(10) gives

$$\sigma_{i,j} = \kappa_i \int \left(\frac{d\eta_{i0}}{dr}\right)^2 dr = \frac{1}{3} \kappa^{1/2} \frac{(2\epsilon)^{3/2}}{\beta}$$

$$= \frac{1}{3} \kappa^{1/2} \frac{2\sqrt{2} \left(\alpha - 2\gamma \sum_{j \neq i}^{p} \eta_j^2\right)^{3/2}}{\beta}$$
 (11)

It has been shown that the interfacial energy is proportional to $\kappa^{1/2}$ and decreases with the parameter γ .

3.2 Visualization of microstructural evolution

To visualize the microstructure evolution using the orientation field variables, the following function was defined:

$$\varphi(r) = \sum_{i=1}^{p} \eta_i^2(r) \tag{12}$$

An example of microstructural evolution in a system with 256x256 cells is shown in Fig. 3. The bright regions are grain interiors and dark lines are grain boundaries. Furthermore, the line profile of φ along the center line of Fig.3 is shown in Fig. 4. It is clear that the value of φ is 1.0 inside the grains, and significantly smaller at grain boundaries. If the grain size is large enough, and only two variables dominate the microstructure, the depth and the width of the potential wells remain constant. The average grain area as a function of time steps for the 512x512 system is shown in Fig. 5. Excluding

the early stage, the average area is found to be proportional to time. The grain size distribution obtained from the 512x512 system is shown in Fig. 6. After a short transient time, the grain size distribution becomes time-independent. As shown in Fig. 7. this size distribution function is in good agreement with that obtained by the Monte Carlo Simulation based on Potts model for two dimensional trianguler lattice. ²⁰⁾

3.3 The effect of variable κ on grain growth

Next, to investigate the effect of κ which is the coefficient of $(\nabla \eta)^2$ term, we performed calculation in which the value of γ was fixed to be $\gamma=1$ and the value of κ was changed from 1.0 to 3.5 with step of 0.5. The effect of κ on the time dependent of average grain area is shown in Fig. 8. The microstructions at t=5000 are shown in Fig. 9, The profiles of φ along with the center lines of Fig.9 are shown in Fig. 10. According to the mean field theory of interface motion, 3) the boundary velocity, V, is generally written as

$$V = B\sigma\Omega(\lambda_1 + \lambda_2) \tag{13}$$

where B is mobility, σ is the boundary energy, Ω is the atomic volume, and $(\lambda_1 + \lambda_2)$ is the mean curvature. The relationship between κ and the square of growth rate nomalized at $\kappa = 2.0$ is shown in Fig. 11. According to eq.(11), we can say, σ is proportional to the square root of κ . This indicates that the result shown in Fig. 11 is in good agreement with the mean field theory. Figure 10 indicates that the thickness of grain boundary becomes broader with the increase of the value of κ . Thus the growth rate increases with the value of κ . In cases of $\gamma = 1.0$ or 1.5, eq.(11) is not allways valid because the interface region which is dominated by only two variables is too small to detect.

Since the change of κ affects growth rate, the time steps taken to reach the scaling region are dominated by the value of κ . However the size distribution and the side distribution functions in the scaling region are time-invariant. These results are in good agreement with these obtained by the Monte Carlo simulation. ²¹⁾

3.4 The effect of variable γ on grain growth

To investigate the effect of γ on growth kinetics we performed calculations in which $\kappa=2.0$ were fixed and the value of γ was changed from 0.6 to 3.0. The effect of γ on the dependence of average grain area is shown in Fig. 12. The microstructures at t=10000 are shown in Fig. 13. The profiles of φ along the center line of Fig. 13 is shown in Fig. 14.

According to Fig. 14, we can find the fact that, the larger the value of γ is, the deeper and sharper the shape of surfaces becomes. In the case of $\gamma=3.0$, it is difficult to evaluate the width of the interface. Because the portion of interface region which is dominated by only two variables is too small to detect. The contribution to σ of the gradient energy term becomes smaller with the increase of the diffuseness of interface. But the decrease in energy can only be achieved by introducing more material at the interface. ¹⁸⁾ As shown in Fig. 15, in the region which the approximation of eq.(9) is applicable, the smaller γ becomes, the larger the value of σ will be. And the fact is in good agreement with the result shown in Fig. 12.

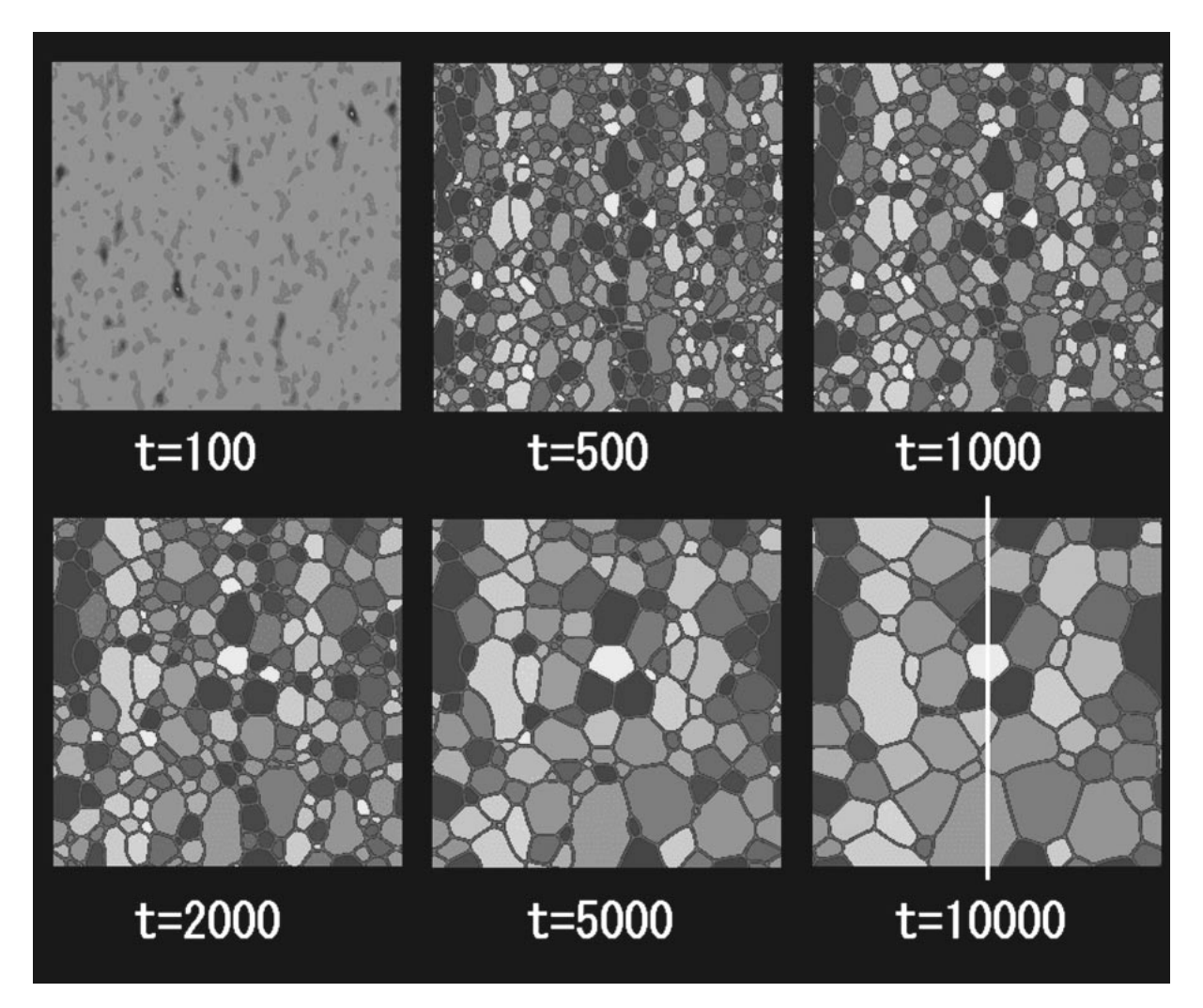


Fig. 3 Microstructural evolution in the 256x256 cells.

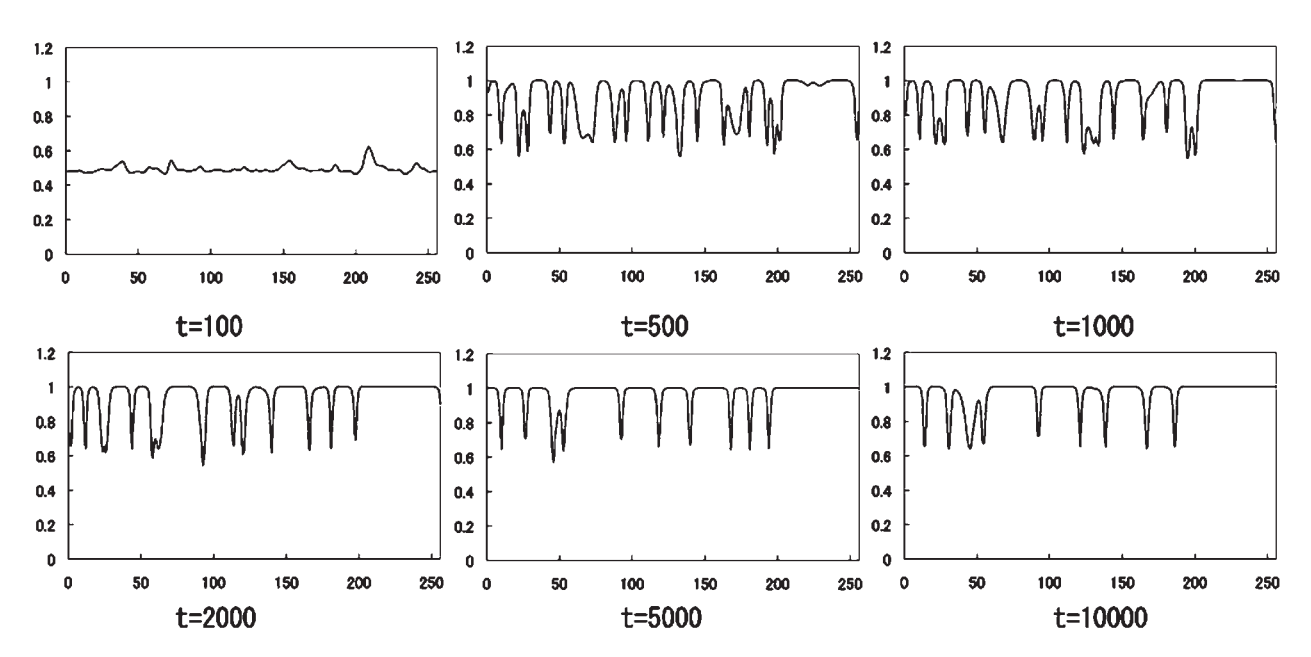


Fig. 4 Line profiles of a function φ along the center lines of Fig.3.

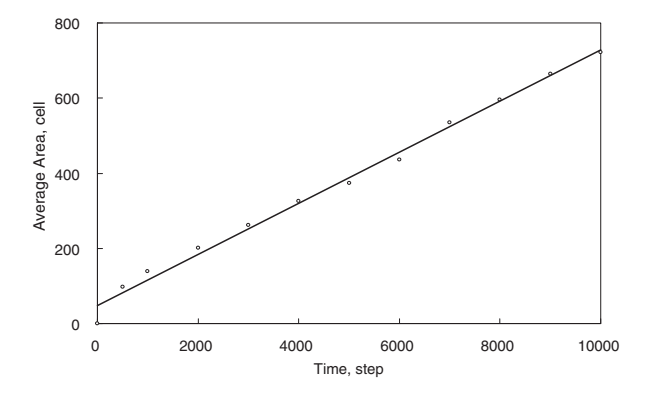


Fig. 5 Average area versus time steps.

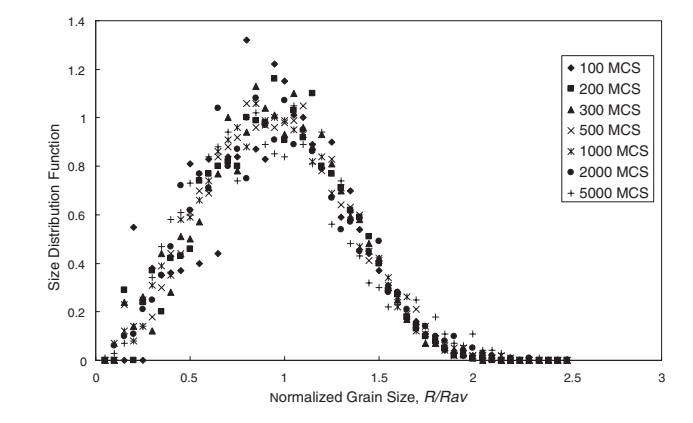


Fig. 7 Variation of the scaled grain size distribution function with time(Calculated by Monte Carlo Simulation)

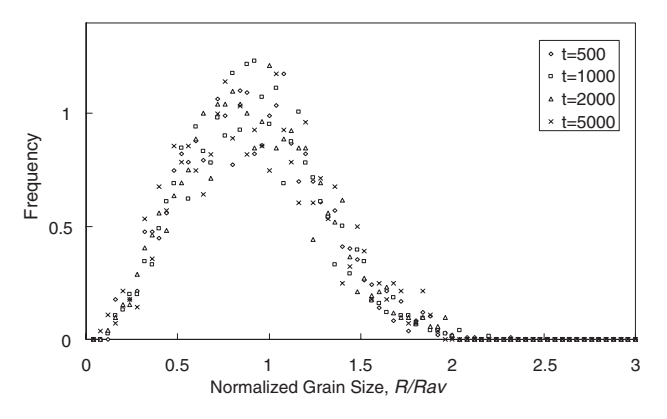


Fig. 6 Variation of the scaled grain size distribution function with time.

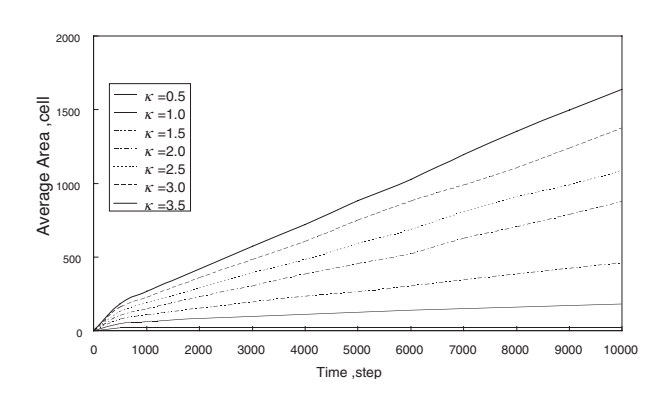


Fig. 8 Effect of a parameter κ on the time dependence of average area.

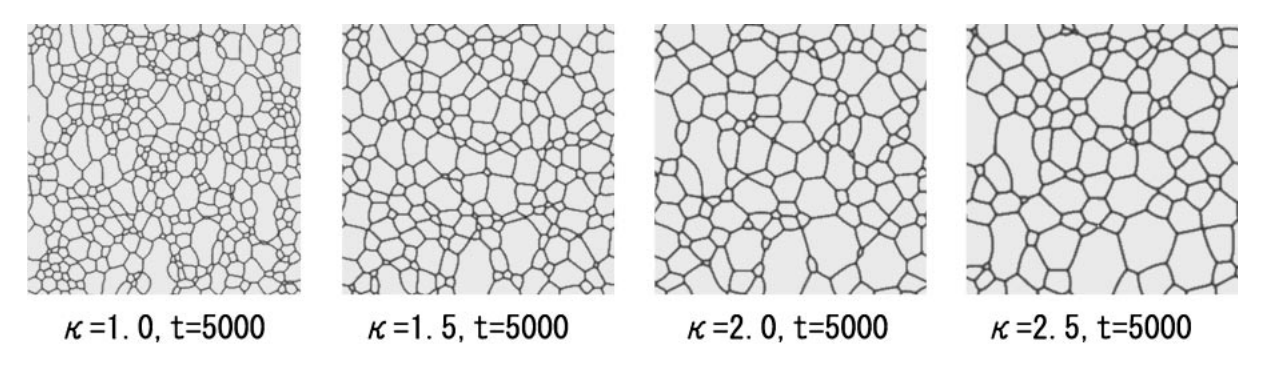


Fig. 9 Effect of a parameter κ on the microstructure at t=5000.

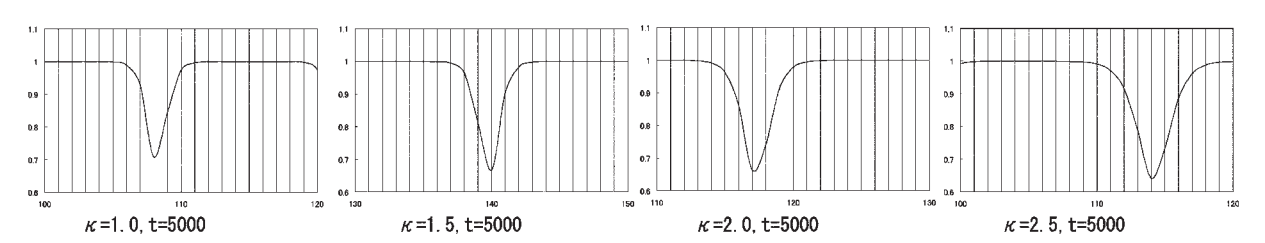


Fig. 10 Line profiles of a function φ along the center lines of Fig.9.

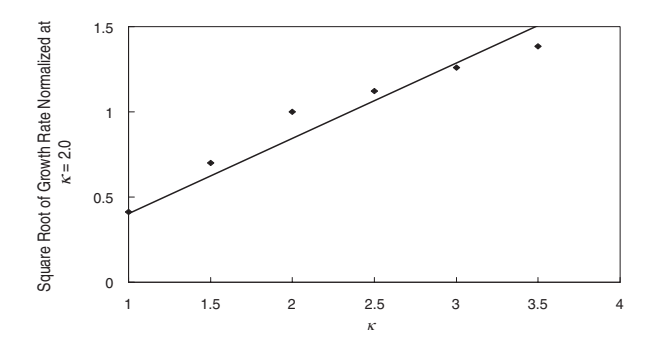


Fig. 11 Relationship between a parameter κ and the square root of normalized growth rate.

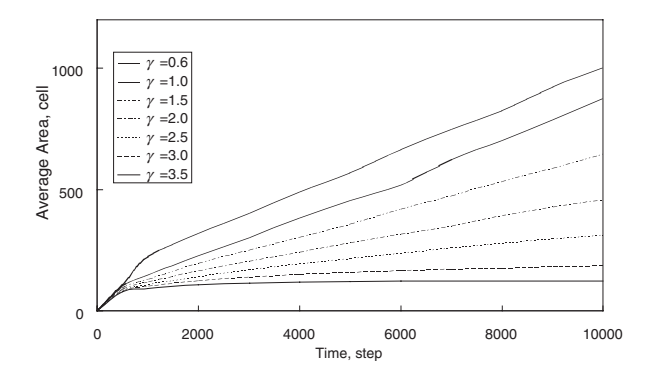


Fig. 12 Effect of a parameter γ on the time dependence of average grain area

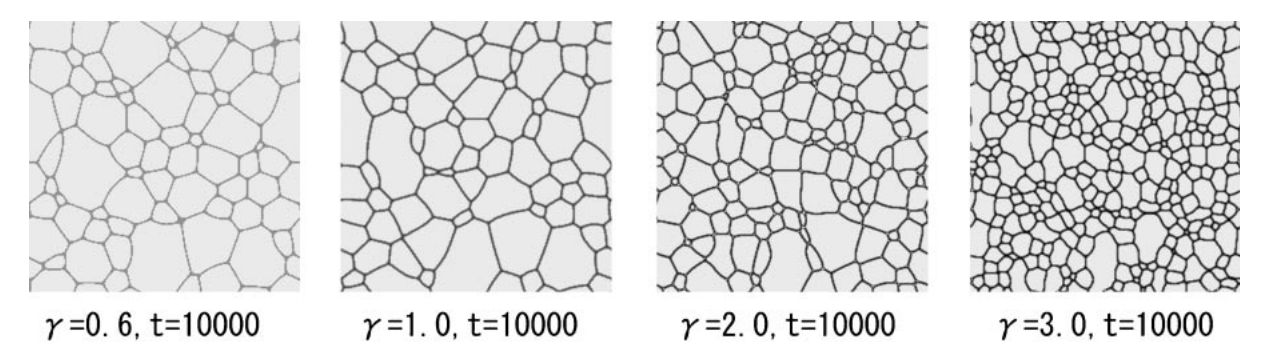


Fig. 13 Effect of a parameter γ on the microstructure at t=10000.

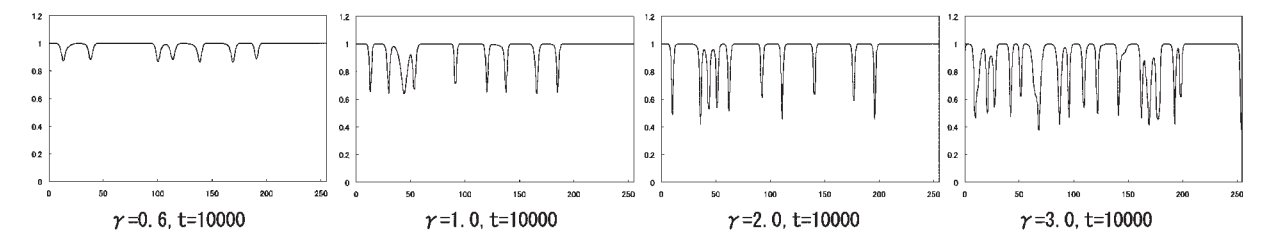


Fig. 14 Line profiles of a function φ along the center lines of Fig.13.

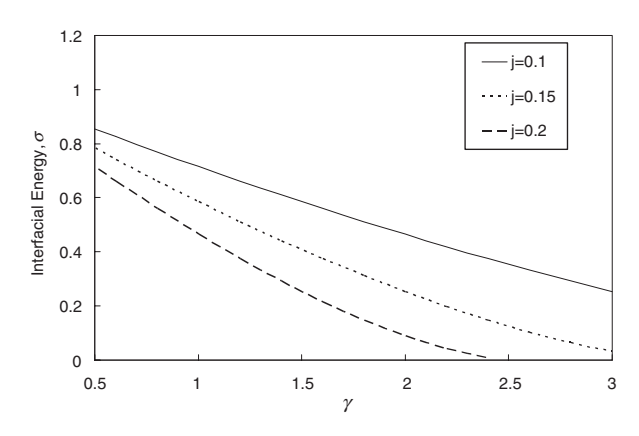


Fig. 15 Effect of a parameter γ on the interfacial energy σ .

Since the change of γ affects growth rate, the time steps which taken to reach the scaling region is dominated by the value of γ . But the size distribution and the side distribution functions in the scaling region are time-invariant.

4. Conclusions

Numerical simulation of grain growth based on the phase field method were performed in order to investigate effect of interfacial energy on kinetics of growth. The following results are obtained.

- Based on the analysis of the stationary solution of the kinetic equation describing grain growth, it has been shown that the gradient energy coefficient κ , and a parameter γ in a local free energy function affects interfacial energy of a materials, σ .
- The average size is proportional to the square root of time. After a short transient time, the grain size distribution and the grain side distribution functions become time-independent. These results are in good agreement with these obtained by the mean field theory and the Monte Carlo simulation.
- Growth rate becomes larger with the increase of κ . And growth rate becomes smaller with the increase of γ . These results are in good agreement with these obtained by conventional theories.

Acknowledgements

The authors are grateful to Ms. Kanako Goto for her help in preparing a manuscript.

REFERENCES

- 1) H.V.Atkinson: Acta Metall. 36 (1988) 469-491.
- 2) D.Weaire and J.A.Glazier: Mater. Sci. Forum 94-96 (1992) 27-38.
- 3) M.Hillert: Acta Metall.13 (1965) 227-238.
- 4) J.E.Burke and D.Turnbull: Prog. Metal Phys.3 (1952) 220-292.
- 5) N.P.Louat: Acta Metall. 22 (1974) 721-724.
- 6) D.Weaire and F.Bolton: Phys. Rev. Lett. 65 (1990) 3449-3451.
- 7) D.Weaire and J.P.Kermode: Philos. Mag. B48 (1983) 245-249.
- 8) D.Weaire and H.Lei: Philos. Mag. Lett. 62 (1990) 427-430.
- K.Kawasaki, T.Nagai and K.Nakashima: Philos. Mag. **B60** (1989) 399-421.
- 10) C.V.Thompson, H.J.Frost and F.Spaepen: Acta Metall. 35 (1987) 887-

890

- M.P.Anderson, D.J.Srolovitz, G.S.Grest and P.S.Sahni: Acta Metall. 32 (1984) 783-791
- D.J.Srolovitz, M.P.Anderson, P.S.Sahni and G.S.Grest: Acta Metall. 32 (1984) 793-802
- D.Raabe: Computational Materials Science: the Simulation of Materials Microstructure and Properties, (Wiley. VCH, Weinheim, 1998) pp.179-199.
- 14) D.Fan and L.Q.Chen: Acta Mater. 45 (1997) 611-622.
- 15) D Fan, C.Geng and L.Q.Chen: Acta Mater. 45 (1997) 1115-1126.
- V.Tikare, E.A.Holm, D.Fan and L.Q.Chen: Acta Mater. 47 (1999) 363-371.
- 17) C.E.Krill III and L.Q.Chen: Acta Mater. **50** (2002) 3057-3073.
- 18) J.W.Cahn and J.E.Hilliard: J.Chem. Phys. 28 (1958) 258-267.
- Y.Saito: An Introduction to the Kinetics of Diffusion Controlled Microstructual Evolution in Materials, (Corona Publishing, Tokyo, 2000) pp. 61-66.
- 20) Y.Saito: Mater. Sci. Eng. A223 (1997) 114-124.
- 21) Y.Saito and M.Enomoto: ISIJ Int. 32 (1992) 267-274.